Self-Assembly of Spherical Particles on an Evaporating Sessile Droplet

Michael Schnall-Levin, Eric Lauga, and Michael P. Brenner*

Division of Engineering and Applied Sciences, Harvard University, Cambridge, Massachusetts 02138

Particles adsorbed on the surface of a droplet form three-dimensional packings when the droplet evaporates. We study the final packings when the liquid droplet is attached to a solid substrate. In contrast to a droplet evaporating away from a substrate, here the final packings are highly dependent on both the number of particles and the contact angle between the droplet and the surface. Simple geometrical constraints quantitatively determine the parameter regions that particular packings can form.

I. Introduction

Perhaps the most natural strategy for self-assembly is to design an energy landscape so that the desired outcome is the energy minimum.[1,2] The primary difficulty with this strategy is the prevalence of local minima. For example, if we consider clusters of N particles interacting through a van der Waals potential, the number of local minima increases from at least 4 for $N = 7$ to 988 for $N = 13$.[3] For this reason, successful assembly strategies have generally employed patterned surfaces or templating strategies to lower the number of local minima.[4−9] It therefore came as a surprise when Manoharan et al.[10] demonstrated a method employing no patterning or templating for forming large numbers ($\sim 10^{10}$) of unique packings of micron-scale particles, with no observable multiplicity of structures. Their method used polystyrene spheres in an emulsion of toluene and water, in which the toluene was then preferentially evaporated. Due to surface tension, the spheres lay at the interface between the toluene and water and as the droplets evaporated, the spheres came together to form unique packings.

How did this method eliminate the local energy minima? The uniqueness of the final structures arises from two features of the assembly process:[11] (1) The particles are initially confined on the two-dimensional surface of the toluene droplet. As the droplet evaporates, the particles become jammed together and the droplet cannot evaporate further while maintaining a spherical shape. The configuration in which they are jammed together is in fact unique.[11−13] Henceforth, we call this particle configuration the initial packing. (2) When the droplet evaporates further, it cannot maintain its spherical shape, and hence the initial packing must deform. However, the final packing of the spheres (when the

toluene has completely evaporated) is uniquely related to the initial packing of the particles: the kinematics of particle contacts as well as the mechanical equilibrium of individual particles do not allow any freedom among the particle contacts once they are initially jammed together.

The extreme nonuniqueness of the self-assembly of three-dimensional particle clusters is eliminated by first confining the particles to a closed surface of lower spatial dimensionality, where the minimal energy structures are completely unique, and then deforming this surface until geometrical constraints prohibit further deformation. The final assembled morphology (the final packing) is then completely determined by the initial packing (though in general the final packing is different than the initial one).

The challenge now is to figure out whether this assembly strategy can be suitably generalized to allow tuning of the final packings. The observed unique map between the final packing and the initial packing implies that the assembly strategy must focus on tuning the initial packings. One method for changing the initial packing is to introduce particles with different wettabilities.[11] Here we explore another possibility, the effect of an external geometrical constraint. Instead of allowing the evaporating droplets to float freely in the bulk, we constrain them in this paper to sit on a surface, with a fixed contact angle during evaporation, α, as illustrated in Figure 1.

We find that for this problem multiple final packings are allowed for a given N. The packings that can form depend strongly on both α and N: For low contact angles and particle numbers, we find that the final packings are either planar (with only a single layer of particles on the solid surface) or highly symmetric. In contrast, at high contact angles and high particle numbers, the packings are generically highly distorted, with no apparent symmetries. We present a quantitative explanation for this transition using geometric constraints on the initial packings.

II. Initial Packings

Our numerical study builds on the background discussed above.[11] When the liquid droplet is sufficiently large, the particles do not touch. In this regime, the minimum energy configuration requires that the droplet is a spherical section. This minimum energy solution holds until the particles jam together at a critical liquid volume V_*. When jamming occurs, it is no longer possible to shrink the liquid volume while maintaining the liquid surface as a spherical section.

This observation naturally breaks the problem of computing the final packings into two parts: First, we need to find the

* To whom correspondence should be addressed.

(1) Whitesides, G. M.; Boncheva, M. *Proc. Natl. Acad. Sci. U.S.A.* **2002,** *99,* 4769.
(2) Whitesides, G. M.; Grzybowski, B. *Science* **2002,** *295,* 2418.
(3) Hoare, M.; McInnes, J. *Faraday Discuss. Chem. Soc.* **1976,** *61,* 12.
(4) Kralchevsky, P. A.; Denkov, N. D. *Curr. Opin. Colloid Interface Sci.* **2001,** *6,* 383.
(5) Yin, Y. D.; Lu, Y.; Gates, B.; Xia, Y. N. *J. Am. Chem. Soc.* **2001,** *123,* 8718.
(6) Lee, I.; Zheng, H. P.; Rubner, M. F.; Hammond, P. T. *Adv. Mater.* **2002,** *14,* 572.
(7) Xia, Y. N.; Yin, Y. D.; Lu, Y.; McLellan, J. *Adv. Funct. Mater.* **2003,** *13,* 907.
(8) Gates, B. D.; Xu, Q. B.; Love, J. C.; Wolfe, D. B.; Whitesides, G. M. *Annu. Rev. Mater. Res.* **2004,** *34,* 339.
(9) Wang, D. Y.; Mohwald, H. *J. Mater. Chem.* **2004,** *14,* 459.
(10) Manoharan, V. N.; Elsesser, M. T.; Pine, D. J. *Science* **2003,** *301,* 483.
(11) Lauga, E.; Brenner, M. P.; *Phys. Rev. Lett.* **2004,** *93.*
(12) Clare, B. W.; Kepert, D. L.; *Proc. R. Soc. London A* **1986,** *405,* 329.
(13) Kottwitz, D. A. *Acta Crystallogr. Sect. A* **1991,** *47,* 158.
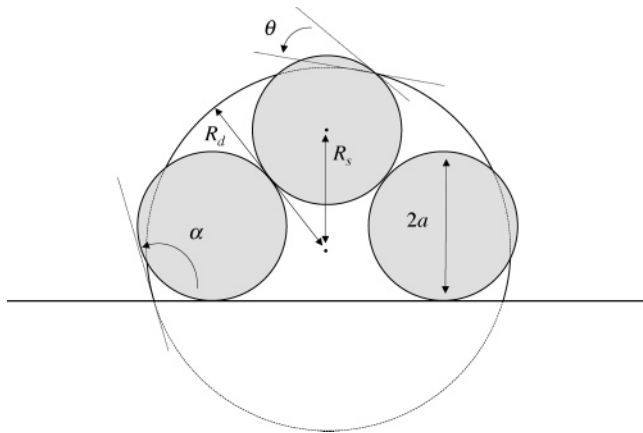
Figure 1. Schematic representation of the proposed experiment. A number N of spherical particles of radius a (here $N = 3$) are adsorbed at the surface of a sessile droplet of solvent on a solid substrate. The contact angle between the droplet and each particle is θ and that between the surface and the droplet is α. At the initial jamming stage (see text for definition), we denote by R_d the radius of the droplet and by R_s the distance between the center of the droplet and the center of the particles.

particle configurations at the critical liquid volume where the initial jamming occurs. Then we need to find out how these initial packings deform during the rest of the evaporation. Given that the final packing is uniquely determined by the initial packing,[11] we can get a good idea of the landscape of possibilities by first examining the initial packings, a task to which we now turn.

A. Numerical Method. The initial packings are equivalent to the jammed packings of circles on a spherical cap resting on a solid surface with a prescribed contact angle. (The set of jammed packings contains the set of densest packings but may also contain others.) The method most commonly used for finding densest packings of circles on a sphere has been to assign a steep repulsive energy between the circles, and use a gradient descent method to minimize this energy.[13] Instead, we use a Markov Chain Monte Carlo algorithm with simulated annealing, first suggested by Krauth.[14] In the algorithm, an initial angular randomized configuration of circles is generated and placed on a sphere of sufficient size that none of the circles overlap. Then the algorithm iterates, at each step picking one of the circles at random and attempting to move it in a randomly chosen direction. If the move is allowed without violating nonoverlap constraints, it is made, otherwise the move is not made. At regular multiples of iterations, a simulated annealing is attempted, in which the radius of the sphere is decreased by a small fraction, and the nonoverlap constraints are checked. Again, if the annealing is allowed without violating any of the constraints, it is completed, otherwise it is not. The annealing step represents the evaporation of the droplet. These random motions and annealings are repeated a large number of times. In our simulations, we performed typically 100 000 random motions with an annealing at every 10th motion (with the choice of annealing at every 10th motion made from a balance to avoid extra computation) and then the size of the random motion, and the fraction of the sphere radius decrease in the annealing step, are decreased and the iterations repeated. (Typically, we decrease each of these by factors of 10, until round off error sets in.) We have tested this algorithm up to $N = 20$ on the problem of packing circles on free spheres and have found all of the known densest packings and features (including the presence of "rattlers" (particles whose centers are not fully

constrained) at $N = 5$ and $N = 19$, and the two different densest packings at $N = 15$, see ref 13), so we are confident in the general accuracy of this method.

The algorithm has two major advantages for our purposes over the traditional gradient descent method. The first is that, since the algorithm explicitly checks that nonoverlap constraints are satisfied, moving to different geometries is an extremely straightforward modification. The second is that the algorithm more closely reflects the experimental reality that we aim to capture in solving the densest-packing problem: the Brownian motion of particles with the slow evaporation of the sphere on which they rest. Because of this, the algorithm will find all of the jammed packings of circles (not just the densest packings) and thus all of the corresponding initial packings of spheres.

We end our description of the algorithm by noting that on a ~1 GHz computer a single run of the algorithm takes a few minutes (for typical values of $N \sim 10$). The running time of the algorithm is ostensibly $O(N)$ since at every iteration only the distances between the one circle being moved and every other circle must be checked (and at every annealing only the two closest circles must be checked to check if constraints are still satisfied); however, the number of iterations required to achieve a jammed packing with probability close to 1 must be increased with increasing N, making the running time longer than $O(N)$.

B. Packing Results. Our algorithm to find initial packings was run for the number of particles N, from 4 to 12, and for contact angle between the droplet and surface α, from $3\pi/16$ to π. For our computations, we restricted our attention to the contact angle between the particles and the liquid, θ, being fixed at $\pi/2$. [In the analytical results below, we generalize to arbitrary valued θ.]

The results of our packing simulations are displayed in Figure 2. Two features of our packing results are particularly notable. The first is that, unlike the case of packing circles on free spheres, multiple jammed packings were found that were not the densest packings, even at low N.[2] The second feature of note is that for low values of N ($N < 9$), the inital packings found are all highly symmetrical below a critical value of α (the added constraint of the surface is most dominant for low α). For α below this critical value, the packings found are either a ring structure, where all of the circles lie on the plane of the surface in a single ring, or a pyramid structure, where $N - 1$ of the particles lie in a ring and one particle rests on top of the others. Examples of these two structures for different values of N are shown in Figure 3.

At α above the critical value, the packings found are rather asymmetric. Some examples of these structures are shown in Figure 4.

III. Final Packings

What happens to the initial packings upon further drying? To determine this, we carry out numerical simulations of the full drying process using the Surface Evolver,[15] a program which determines the equilibrium configuration of deformable surfaces given the definition of an energy. The colloidal spheres are modeled as liquid droplets with high surface tension, typically 1−2 orders of magnitude larger than the main droplet, to penalize nonspherical deformations of their shape. Interfacial tension

(14) Krauth, W. *Markov. Processes Relat. Fields* **2002**, *8*, 215.

(15) Brakke, K. A.; *Exp. Math.* **1992**, *1*, 141.

(16) In the analytical results below, we generalize to arbitrary valued θ.

(17) When we used our algorithm to reanalyze the case of free spheres, no nondensest jammed packings were found below $N = 10$. For N below 20, even when multiple jammed packings were found, these states only differed by ~1 part in 1000 from the densest packing. This may explain why unique structures were found in the original experiments and simulations: differences of 1 part in 1000 may have been present, but were simply were undetectable.

RINGS

PYRAMIDS

Figure 2. Summary of the results of the initial packing simulations, and comparison with the theoretical predictions, plotted in the (α, N) space, in the case where $\theta = 90°$. Top: Region of parameter space where the rings are predicted to be both possible and jammed (light red), region where other asymmetric structures are obtained in simulation at the jamming stage (red) and regions where both types of packings are possible (dark red). Bottom: Region of parameter space where the pyramids are predicted to be both possible and jammed (light blue), region where other asymmetric structures are obtained (blue) and regions where both are possible (dark blue). In both cases, the dots represent the results of initial packing simulations where rings (pyramids) have been obtained.
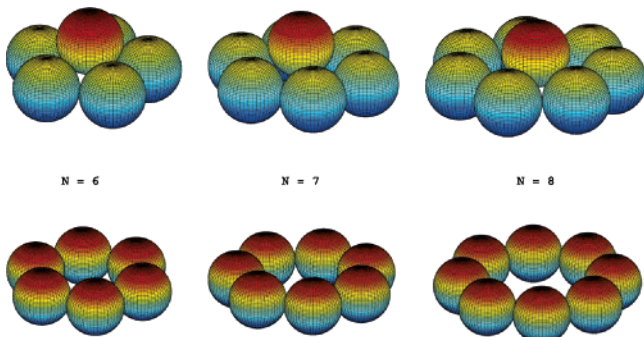
Figure 3. Pyramid and ring initial packings for $N = 6-8$. The pyramid is stable in transitioning to the final packing, while the ring is not.

between the droplet and the particles are chosen appropriately in order to satisfy Young's law at the solid−liquid contact line. Finally, noninterpenetrability is enforced with an excluded volume repulsion energy acting between the centers of the spheres (see ref 11).
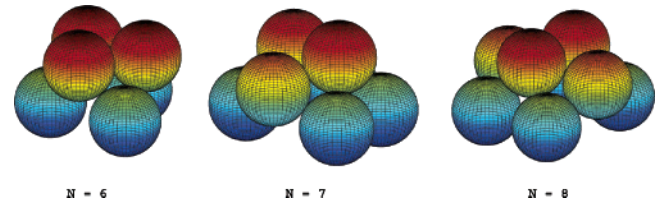
Figure 4. Initial packings obtained when the contact angle with the surface, α, exceeds the critical value, for $N = 6-8$.
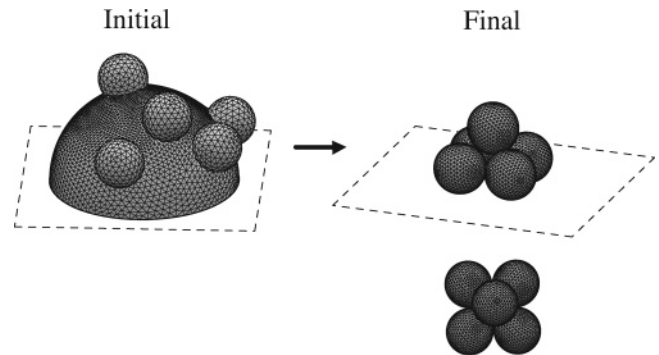
Figure 5. Drying simulation of $N = 5$ spheres on a droplet with $\alpha = \theta = 90°$. Both the initial condition and the final particle configuration (two views) are displayed.

These full simulations are much more computationally intensive than finding the initial packings, so we carry these out only for $N = 5$. The results are illustrated in Figures 5 and 6. Our simulations confirm that both the ring and pyramid occur at the initial packing stage, as described above. Upon further drying, when the droplet evaporates completely, the pyramidal structure remains (see Figure 5). In contrast, the ring structure evolves to a planar symmetric 2−3 configuration (see Figure 6).

What lessons can we extract from these simulations with five particles to the more general case? Although the phase diagrams presented in Figure 1 show only the initial packings, they reflect the morphologies that occur in the final packings. The pyramidal structures are rigid and hence are stable to evaporation. Upon evaporation, the ring-like structures remain planar but deform. Similarly, the disordered structures remain disordered. Hence, Figure 1 illustrates phase boundaries that we expect to be observable in experiments: When N and α are low, the final packings that occur are either planar or pyramidal. Above the critical threshold $N = N^*(\alpha)$, the final packings become disordered. It is noteworthy that for $N < N^*$ multiple equilibria exist for the same (N,α). This occurs because of a degeneracy in the number of initial packings that are accessible to random initial conditions. Although for a given α only one of the structures (ring or pyramid) is the lowest energy state for the initial packing, the other structure may still occur and even may occur more frequently.

IV. Phase Boundary

Given the striking change from ordered to disordered structures at $N = N^*$, it is of interest to understand where this phase boundary comes from. Here we demonstrate that the phase boundary originates from geometrical constraints on when rings and pyramids can form.

The constraints depend on the ratio of the particle radius a to the droplet radius R_d. In what follows, we will nondimensionalize lengths scales by $2a$ so that the particles have radius $1/2$. We use two (dimensionless) variables to describe the size of the structure: r_s is the distance from the center of the droplet to the centers of the particles ($r_s = R_s/2a$), and r_d is the radius of the
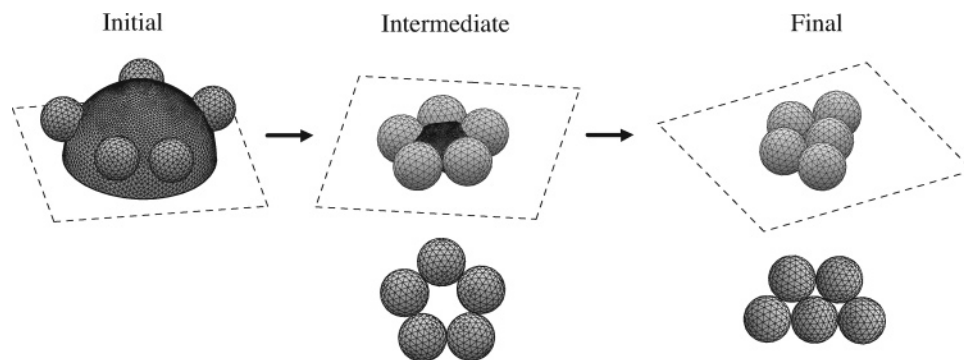
Figure 6. Same simulation as in Figure 5 ($N = 5$, $\alpha = \theta = 90$ °) but with a different initial condition for the particles on the droplet. We display the initial condition, the intermediate packing where the ring structure is obtained (initial packing, two views), and the final packing (two views). The initial ring packing is found to be unstable, and the final assembly of spheres is a planar 2−3 structure.

droplet ($r_d = R_d/2a$). From the law of cosines, it follows that

$$r_s^2 = r_d^2 - r_d \cos\theta + \frac{1}{4} \tag{1}$$

Here θ is the contact angle of the particle-liquid interface. We now consider constraints on forming both rings and pyramids.

A. Constraints on Forming Rings and Pyramids. For the ring structure, two constraints need to be considered: First that the plane the ring lies in is a distance of a particle radius (=1/2) from the surface on which the droplet lies, and second that the radius of the smallest circle on which N points all separated by a distance of 1 can lie, R_N, is the effective radius of the droplet at the ring height. A simple calculation gives that $R_N^{-1} = 2 \sin(\pi/N)$. The condition that the ring lies at a height of 1/2 above the surface implies that

$$\left(\frac{1}{2} + r_d \cos\alpha\right)^2 + R_N^2 = r_s^2 \tag{2}$$

Solving for r_d gives the critical radius of the droplet for the ring structure

$$r_{\text{d, ring}}(N,\alpha,\theta) =$$
$$\frac{\cos\alpha + \cos\theta + \sqrt{(\cos\alpha + \cos\theta)^2 + \sin^2\alpha \csc^2(\pi/N)}}{2\sin^2\alpha} \tag{3}$$

For the pyramid structure, there are now three constraints to consider: The first two are the same as those given above for the $N - 1$ ring (because the pyramid contains the $N - 1$ ring) and the third is that the particle at the top must be a distance of 1 away from particles that lie on the ring. The critical radius is found by solving for at least two out of the three constraints to be satisfied with equality. This gives three possible radii. The actual radius will be the largest of the three radii (since the two smaller radii necessarily violate one of the constraints), subject to jamming conditions discussed below. Letting constraint 1 be that the $N - 1$ ring is a distance of 1/2 from the surface, constraint 2 be that R_N is the effective radius of the droplet at the height of the $N - 1$ ring, and constraint 3 be that the top particle is a distance of 1 from all of the particles in the ring, we find the following. If constraints 1 and 2 are both satisfied with equality, the result is the same as that for the $N - 1$ ring. If constraints 2 and 3 are satisfied at the same time without constraint one being satisfied, the solution cannot be jammed. This is because the $N - 1$ ring is always found to lie in the upper hemisphere of the droplet, and so if it is not resting against the surface, the particles cannot be held in place. The ring can always be brought down and expanded in this case and the constraints relaxed.

Finally, if constraints 1 and 3 are satisfied at the same time, the solution is found to be the positive value of r_d satisfying the following equation:

$$\sqrt{r_d^2 - r_d \cos\theta + \frac{1}{4}} =$$
$$\frac{1 + 2r_d \cos\alpha + \sqrt{4r_d^2 \cos^2\alpha + 4r_d \cos\alpha + 9}}{4} \tag{4}$$

The value of the solution can readily be found numerically. An examination of the graphs of the two sides of the above equation shows that it has always exactly one positive solution for r_d for all values of θ and α (with the exception of the limiting case where $\alpha = \pi$). If we let $r_{13}(\alpha,\theta)$ be the solution of the above equation, then in general we find that the critical radius of the droplet is

$$r_{\text{d,pyr}}(N,\alpha,\theta) = \max\{r_{\text{ring}}(N - 1,\alpha,\theta), r_{13}(\alpha,\theta)\} \tag{5}$$

The above formulas for the critical radii of both structures give values that agree exactly (to the precision of our numerical calculations) with the critical radii of the configurations output by our computations.

B. Jamming. Simple geometric calculations also yield results for whether the structures are jammed. By jammed, we mean that no movement of any of the particles is allowed that would change the structure of the packing: if this is not satisfied, the structure will not be found as an initial packing. (Note that for the pyramid structure this might allow the top particle to rattle.) For the ring to be jammed, it must be impossible for any of the particles to move upward and out of the ring; therefore the ring cannot sit in the lower hemisphere of the droplet. Since the ring must lie at a distance of 1/2 from the surface, we have

$$-r_d \cos\alpha = \frac{1}{2} \tag{6}$$

(α is larger than $\pi/2$ for our limit) and therefore from eq 2, $r_s = R_N$. Using this in eq 1, we find that for the structure to be jammed α must be smaller than a critical value, α_c, given by

$$\alpha_c = \cos^{-1}\left(\frac{-1}{\cos\theta + \sqrt{4R_N^2 + \cos^2\theta - 1}}\right) \tag{7}$$

Whether the pyramid structure is jammed depends on which constraints are being satisfied with equality. If

$$r_{\text{ring}}(N - 1,\alpha,\theta) > r_{13}(\alpha,\theta) \tag{8}$$

then the pyramid structure is identical to the $N-1$ ring structure and therefore is jammed when the $N-1$ ring structure is jammed. For θ fixed at $\pi/2$, examination shows that this is always the case for $N \geq 6$. In the other case, the $N-1$ ring must take up at least half of the angular space so that the top particle cannot drop down. This implies the inequality

$$\sqrt{1 - \frac{1}{4r_{\text{s,pyr}}{}^2}} < \frac{1}{2\,\sin\!\left(\dfrac{\pi}{2(N-2)}\right)} \tag{9}$$

For θ fixed at $\pi/2$, examination shows that this inequality never holds for $N = 4$ and always holds for $N = 5$ (the cases $N \geq 6$ are again covered entirely by whether the $N-1$ ring is jammed). One consequence of this observation is that the pyramid structure is never found for $N = 4$ (as we confirm numerically).

These conditions to provide for the configurations to be jammed allow us to predict the region where rings and pyramids can exist and hence when ordered initial packings can result from this process. We have plotted in Figure 2 the results of our packing simulations together with our theoretical prediction.

In the light regions of Figure 2, we predict the structures to be present, in agreement with the results of our simulations (dots). If the conditions are outside the range of when a given structure will be jammed, that structure will not be present under those conditions, which is also confirmed by our simulations. Note that a given structure satisfying these conditions does not necessarily mean one will typically see it; near the edges of where the structures are jammed we have found the rings and pyramids to appear very infrequently. Finally, we have also plotted in Figure 2 (dark areas) the regions where asymmetric structures such as those present in Figure 4 have been observed in our simulations. These regions intersect both the domains where the

ring and pyramid structure are jammed, indicating the possibility of obtaining both symmetric and asymmetric initial packings.

V. Discussion and Conclusion

A variety of methods have already been proposed to assemble colloidal particles on a template.[5-9] However, these methods rely on the interplay of a liquid with a template whose properties (mechanical, electrical, etc.) have been tuned to obtain a particular structure. In contrast, the method proposed by Manoharan et al.[10] produces unique packings without any templating.

In this paper, we have presented a computational study of an extension of the method in ref 10 when the droplet is fixed on a solid substrate. Most significantly, and unlike the case of a free droplet, a number of different structures are allowed for each value of N. At the jamming stage, we have shown that ring and pyramid structures are prevalent, with the pyramid being stable to subsequent evaporation whereas the rings are not. Furthermore, the distribution of these structures is highly dependent on the contact angle between the droplet and the surface. The results suggest a simple way to control the transition between two-dimensional (planar) and three-dimensional final particle packings.

As an extension, one can envision patterning areas of different structures formed by the above process simply by creating patterns of different wettability on the surface. The algorithm and analytic results given above could aid in the choice of parameters for such an experiment. There are also additional experimental modifications that could be examined using the above algorithm. One such modification would be to look at the case of having two or more different types of particles having different wettabilities.[11]